EGTRIB Journal
JOURNAL OF
THE EGYPTIAN SOCIETY OF TRIBOLOGY
*VOLUME 15, NO. 1, January 2018, pp. 14 - 27* ISSN 2090 - 5882
(Received August 15. 2017, Accepted in final form November 19. 2017)

# STUDY OF DAMPING BEHAVIOR OF RUBBER FLAT WASHERS USING FINITE SELEMENT MODELING

**Rashed A.**

**Production Engineering and Design Department, Faculty of Engineering, Minia University, 61111 Minia, Egypt.**

## ABSTRACT
**The present paper aims to study the damping behavior for different materials of flat washers. Steel as well as rubber washers of different hardness values have been used. The results obtained from the numerical model were found to match experimental results. It was noted that the rubber washers act as an anti-vibration material, where those of 40 Shore "A" hardness gave the best result. Moreover, the stress generated on the rubber washers was less than that observed for steel washer.**

## KEYWORDS
**Anti-vibration, Rubber washer, ABAQUS, Numerical model.**

## INTRODUCTION
**Detection of an antifriction bearing faults is one of the most challenging tasks in bearing health condition monitoring, especially when the fault is at its initial stage. Four different methods for detection and diagnosis of bearing defects; they may be broadly classified as vibration measurements, acoustic measurement, temperature measurements and wear debris analysis have been identified. It is observed that the vibration analysis is most commonly accepted technique due to its ease of application, [1]. Time domain, frequency domain analysis and spike energy analysis have been employed to identify different defects in bearings, [2]. Statistical properties of the vibration signals for healthy and defected structures are compared, [3]. Time-domain parameters such as root mean square (RMS), crest factor and kurtosis are used to analyses the vibration signals, [4 - 6]. The simulated vibration pattern has similar characteristics with results from experimental results, [7]. Then, the model is analyzed to obtain the vibration signal in the frequency domain, [8].**

**Multiple defects are introduced on the outer race of vehicle gearboxes. The effect of the number of outer race defects in deep groove ball bearings are investigated using experimental and numerical methods, [9]. The influence of housing structure with different height 120, 100, 80, 60 and 40 mm is investigated, where the vibration response has been evaluated using the root mean square parameter RMS, [10]. It was found that, the housing with height of 40 mm displayed the lowest fluctuation in the output response.**

**The finite element (FE) model is proposed to study ball bearing with local defect based on the coupling of piecewise function and contact mechanism at the edge of the local defect, [11 - 14]. An analytical model is proposed to study the non-linear dynamic behavior of rolling element bearing systems including surface defects, [15]. The vibrations generated by deep groove ball bearings having multiple defects on races were studied, [16]. The contact pressure distribution between the ball and the raceway of the bearing 6004 is performed by finite element software ABAQUS. To validate the finite element model, an analytical method using Hertzian contact theory is derived by MATLAB software. Influence of shaft misalignment with different angles namely; 0.2°, 0.4°, 0.6°, 0.8° and 1° is investigated, [17]. A simple time series method for bearing fault feature extraction using singular spectrum analysis of the vibration signal is proposed, [18]. The resonance frequency in the first vibration mode of mechanical system was studied, [19]. Under the assumption of a stepwise function for the envelope signal, the modulated signal could be decomposed into a sinusoidal function basis at the first vibration mode resonance frequency. A mathematical model for the ball bearing vibration due to defect on the bearing race has been developed, [20]. Silica sand with different particle sizes and Fe powder all at five concentration levels were used to disperse the lithium grease, [21]. The effect of carbon nanotubes CNTs as lubricant additives was investigated. The vibration amplitude was improved due to increase of concentration of carbon nanotubes CNTs, [22].**

**The current work is carried out to determine the damping characteristics of vibration transfer through deep-groove ball bearings using single ball bearing and the compliance transfer function resulting from the impulses applied to the bearing. Steel washer and rubber washers of different hardness have been used. A three-dimensional model is established to evaluate ball bearing and to obtain simulated vibration signals of housing using FE analysis through ABAQUS software. The vibration monitoring methods are examined using, RMS, root mean square.**

## EXPERIMENTAL

**An experimental setup is employed in this research to collect the vibration signals to study the vibration signatures generated by incipient bearing defects. A sketch of the test rig and the equipment used in collecting the data is shown in Fig. 1. The system is driven three-phase asynchronous motor with cage rotor, with the speed up to6000 r/min. The shaft rotation speed can be controlled by a control unit. An optical encoder is used for shaft speed measurement. Thus, the shaft rotation speed is known directly from the reading of this a control unit. An elastic claw coupling is utilized to damp out the high-frequency vibration generated by the motor.**

**Two ball bearings are fitted into the solid housings. Accelerometers (IMI Sensors-603C01) are mounted on the housing of the tested bearing to measure the vibration signals along two directions. A variable load is applied by a belt drive. A data acquisition card (BMC USB-AD16F) is employed for signal collection.**

**MATERIALS AND METHODS**

**Performance of the device is affected by the magnitude of vibration. The bearing type that has been used in this study is a single row deep groove ball bearing SKF 6004. Lithium grease without additive was used as a basic lubricant. Generally, different materials such as silica sand of (0 - 150 µm) with content ranges from 1 – 5 wt. % of the lithium grease (1.0 g) with step of 1 wt. %. It is obtained that magnitude of vibration depends on or affected by the size and percentage of silica added with the grease to the bearing. Not only contaminants affect the vibration, but also the type of bearing block material. Two types of bearing blocks were used, the first was made of aluminum (one part) and the second was made of steel (two parts are mate by thread fasteners and 5 types of washers). All the bearings were operated for 3 hours at the same speed of 1500 rpm and under the constant radial load of 100 N. Steel and rubber washers used to study their effect on damping of vibration are:**

1- **Steel washer as specimen test "S01"**
2- **Rubber washer (30 Shore A) as specimen test "S02"**
3- **Rubber washer (40 Shore A) as specimen test "S03"**
4- **Rubber washer (50 Shore A) as specimen test "S04"**
5- **Rubber washer (60 Shore A) as specimen test "S05"**

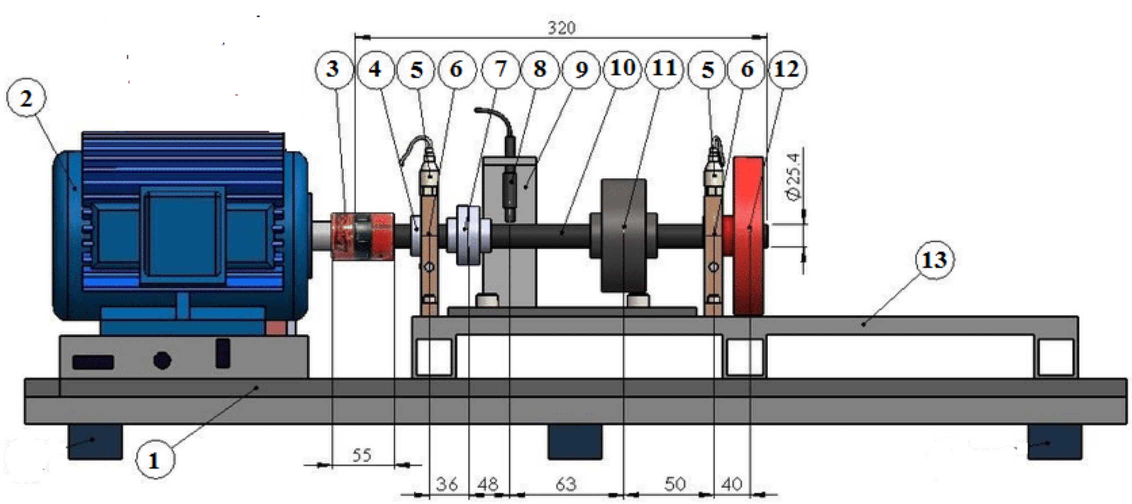


1.Base.
2.Drive unit.
3.Elastic claw coupling.
4.Setting ring.
5.Acceleration sensor.
6.Bearing support "Washer"
7.Coupling
8.Reference sensor.
9.Reference sensor stand.
10. Shaft
11. Loading disk
12. Belt drive.
13. Extended rotor disk.

**Fig. 1 Schematic representation of the test rig.**

## DYNAMIC LOAD ANALYSIS

**In this study, a 6004-model single row deep groove ball bearing of stationary outer race and its housing are considered. It is assumed that the contact between the outer surface of the outer race and its mating surface on the casing structure is perfect meaning that no relative motion permitted on the contact surface. The three-dimensional model of the housing and outer race is modeled in commercial package ABAQUS/CAE. The housing model is created according the dimensions shown in Fig. 2. The outer race dimensions of the SKF 6004 ball bearing are used. It is assumed also that, the bearing material is isotropic and linear-elastic fracture mechanics with modulus of elasticity "E" of 196 GPa, Poisson's ratio "ν" of 0.28 and density "ρ" of 7800 Kg/m$^3$. For the housing, the material is assumed to be isotropic and linear-elastic fracture mechanics with modulus of elasticity "E" of 70 GPa, Poisson's ratio "ν" of 0.35 and density "ρ" of 2700 Kg/m$^3$. For the steel washer, the material is assumed to be isotropic and linear-elastic fracture mechanics with modulus of elasticity "E" of 190 GPa, Poisson's ratio "ν" of 0.3 and density "ρ" of 7700 Kg/m$^3$. For the rubber washer, the material is assumed to be isotropic and linear-elastic fracture mechanics with modulus of elasticity "E" of 1.4 MPa, Poisson's ratio "ν" of 0.499 and density "ρ" of 1100 Kg/m$^3$. The elements of a rolling element bearing have different frequencies determined by the shaft frequency and geometry of the bearing. The frequencies are cage frequency "$f_c$" and rolling element frequency "$f_r$". The inner ring rotates with shaft frequency "$f_s$". The cage and rolling element frequency are given by the following expressions for a bearing having a stationary outer ring.**

$$f_c = \frac{f_s}{2}\left(1 - \frac{D}{d_m}\cos\alpha\right) \qquad (1)$$

$$f_r = \frac{d_m f_s}{2d_b}\left(1 - \frac{D^2}{d_m^2}cos^2\,\alpha\right) \qquad (2)$$

**Where, "$f_s$" is the shaft frequency in Hertz, "α" is the contact angle which is taken as 0˚. The loads carried by the ball and roller bearings are transmitted through the rolling elements from one race to the other. The relationship between load and deflection is:**

$$Q = K\delta^n \qquad (3)$$

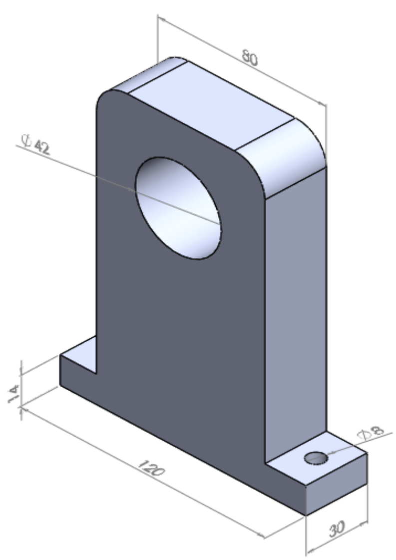


**Fig. 2 Basic dimensions of the housing structure.**

**Where, "n" = 1.5 for ball bearings and "n" = 1.11 for roller bearings, "Q" is the ball or roller normal load, "δ" is deformation, and "K" is load-deflection factor.**

**For a rigidly supported bearing subjected to a radial load, the radial deflection at any rolling element angular position is given by:**

$$\delta_{\psi} = \delta_{max}\left[1 - \frac{1}{2\,\varepsilon}(1-\cos\psi)\right] \quad (4)$$

$$\varepsilon = \frac{1}{2}\left(1 - \frac{P_d}{2\,\delta_r}\right) \quad (5)$$

**Where, "$\delta_r$" is the race radial shift, occurring at $\psi = 0^0$, "$P_d$" is the diametric clearance, "ε" is the load distribution factor.**
**The angular extent of the load zone is determined:**

$$\psi_l = \cos^{-1}\frac{P_d}{2\delta_r} \quad (6)$$

**For ball bearings having zero clearance and subjected to a simple radial load determined that:**

$$Q_{\psi} = Q_{max}\left[1 - \frac{1}{2\,\varepsilon}(1-\cos\psi)\right]^n \quad (7)$$

$$Q_{max} = \frac{4.37\,F_r}{Z\cos\alpha} \quad (8)$$

**Where, "$F_r$" is radial load and "Z" is number of balls.**
**The contact between the rolling elements and the outer race occurs in a small area under loading. Dynamic excitation of the bearing structure is established by means of applying the radial load calculated from Eq. (7) on each node along the inner circumference of the loading zone. Duration of the impacts is determined by the rotational speed of the shaft. A radial force is defined due to the assumption of the contact area. As result of the contact that is assumed to be point contact, the acting magnitude force is assumed square form, as shown in Fig. 3.**

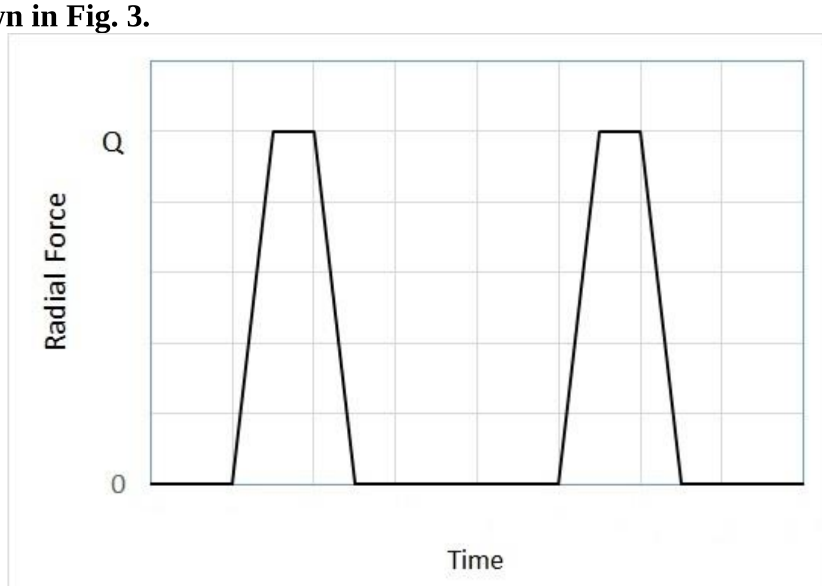


**Fig. 3 Constant radial load acting on a contact area.**

## RESULTS AND DISCUSSION

### VIBRATION SIGNATURES ANALYSIS

**The damping ratio is a dimensionless measure describing how oscillations in a system decay after a disturbance. Many systems exhibit oscillatory behavior when they are disturbed from static equilibrium position. A mass suspended from a spring, for example, might, if pulled and released, bounce up and down. On each bounce, the system tries to return to its equilibrium position, but overshoots it. Sometimes, losses (e.g. frictional) damp the system and can cause the oscillations to gradually decay in amplitude towards zero or attenuate. The damping ratio is a measure of describing how rapidly the oscillations decay from one bounce to the next.**

**In this section, the vibration damping is analyzed for rubber and steel washers to investigate their effectiveness in damping bearings. Figure 4 illustrates the effect of different washers on damping of vibration in bearing greased by lithium grease contaminated by 1 wt. % silica of single cut of 150 µm particle size. The vibration data was carried out under shaft rotational speed of 1500 rpm. The figure shows that the amplitude of vibration always in the rubber washers depends on the hardness and the highest value of the vibration amplitude occurs in steel washer.**

**The measurement of the system response of the different types of washers when lithium grease was dispersed by silica additives as contamination is discussed. The damping ratio is a measure of describing how rapidly the oscillations decay from one bounce to the next. Fig. 5 shows the relation between the acceleration amplitude, with 1 wt. % of silica added to lithium grease, versus time for different types of washers. It is shown that the relation between rubber hardness and acceleration amplitude (RMS) is not linear, where rubber of 30 shore A hardness gives almost behavior of 50 shore A. The rubber washer of 40 shore A hardness gives the lowest acceleration amplitude at different times, while the highest value occurs when using steel washer at deferent times. Figures 6, 7 illustrate the relation between the acceleration amplitude with 3 and 5 wt. % of silica added to lithium grease respectively. It was found that the steel washer S01 has the highest value of acceleration amplitude RMS for all silica additives percentages.**

**Moreover, the rubber washer S03 has the lowest value of acceleration amplitude RMS, as shown in Fig. 8. It is noticed that rubber washer 40 shore A, S03, has the favorable damping factor of vibration due to its favorable hardness so it gives the best result. The steel washers give the highest value of acceleration amplitude at all concentration of silica additives. It can be recommended that rubber washer S03 is good anti-vibration material that possesses high damping factor that does not increase greatly with frequency.**

### SIMULATION RESULTS ANALYSIS

**The analytical result describes the alteration of the bearing acceleration, velocity and displacement. Figure 9 illustrates the dynamic model used to study the damping factor of different washers. The variation of the RMS of the acceleration versus the shaft speed was shown in Fig. 10. The value of the RMS at point ''$P_1$'', i.e. in the vertical direction is small in comparison to the horizontal one.**

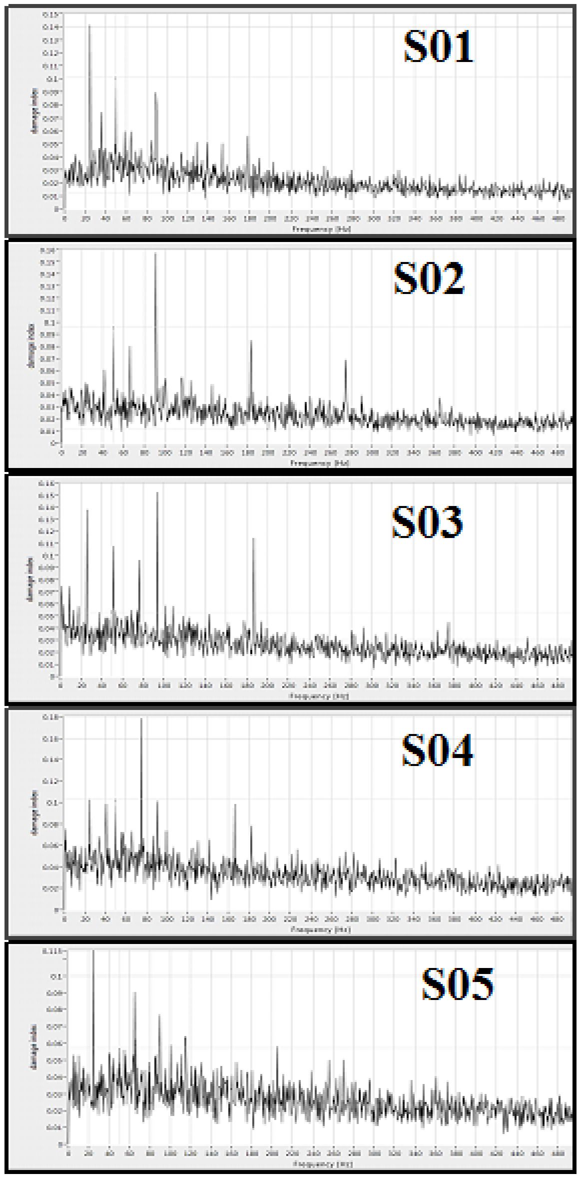


**Fig. 4 Experimental acceleration response for healthy bearing and bearings contaminated by 1 wt. % silica size (0- 150 μm).**

**In addition to that, the RMS decreases with the increase of the shaft speed. The comparison between the simulation and experiment results shows good agreement between the results. Besides, the model may be used to determine the generated stresses on the outer race of ball bearing and the washers. Figure 11 illustrates the maximum principle stresses generated on the outer race of ball bearing. It is found that the maximum stress is $2.9 \times 10^6$ Pa at the center of the race and the stress distribution around of the half of the race. Figures 12, 13 show that the generated stresses on the steel washer is higher than that observed on the rubber one. It may be due to the damping factor of rubber is being higher than the damping factor of steel. It was observed that the stresses generated on the steel washer are concentrated on the inner edges. Furthermore, the stresses generated on the rubber washer are distributed on the upper surface. It seems**

that the rubber is more ductile than the steel that allows the material to absorb the generated stresses.

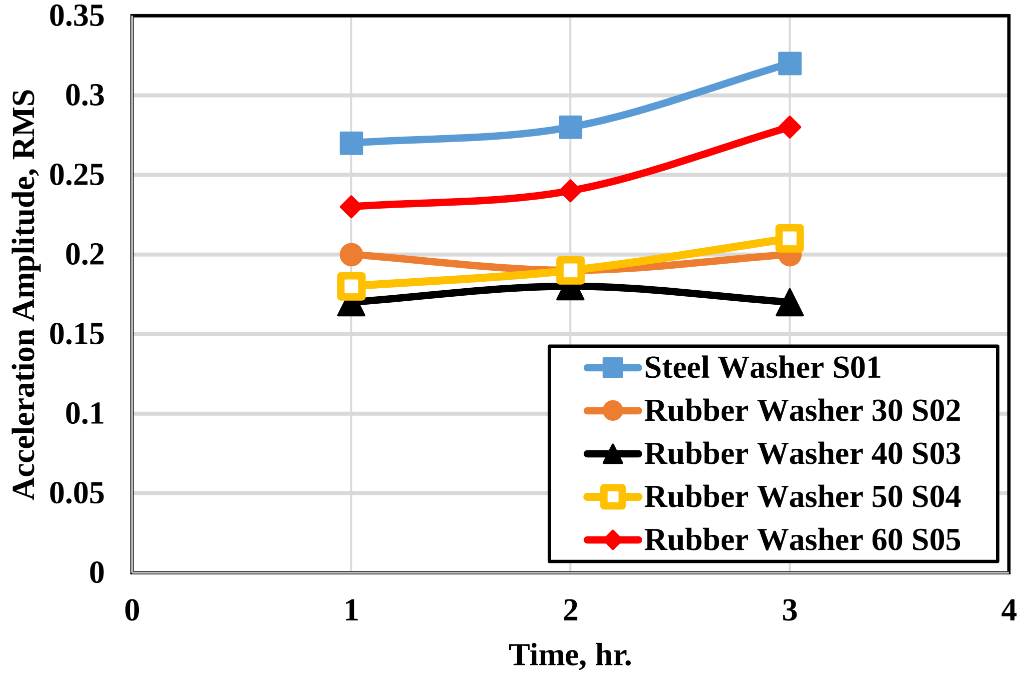


Fig. 5 Acceleration Amplitudes relationship with additives silica of 1 wt. % of different washers.

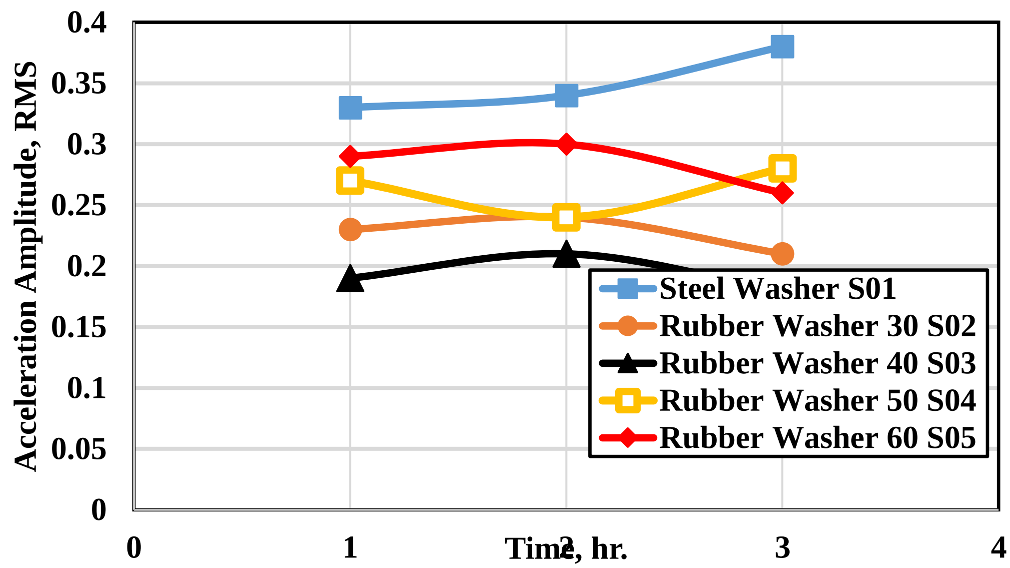


Fig. 6 Acceleration Amplitudes curve with additives silica of 3 wt. % of different washers.

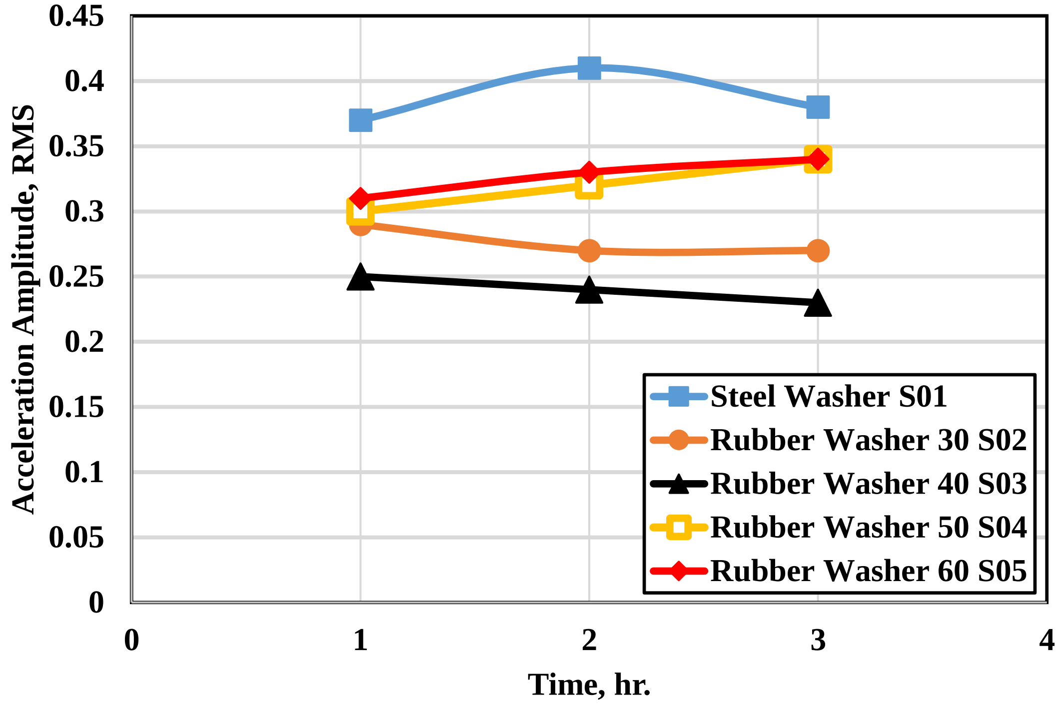


**Fig. 7 Acceleration Amplitudes curve with additives silica of 5 wt. %of different washers.**

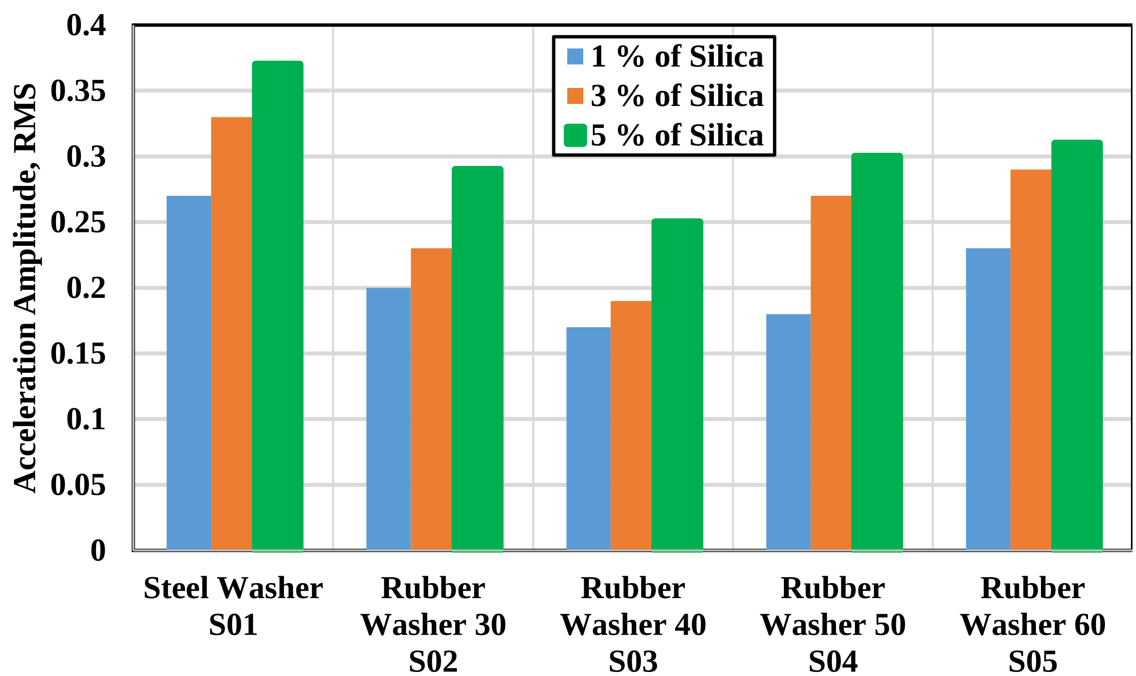


**Fig. 8 Comparison of acceleration amplitudes of different washers after 1 hr.**

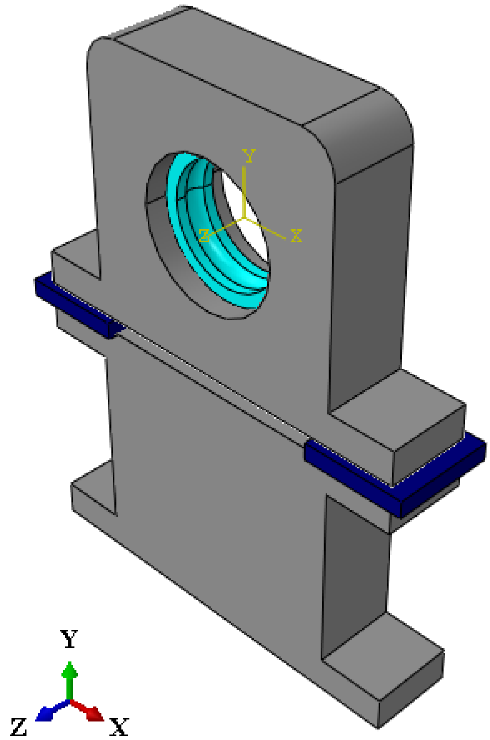


Fig. 9 Finite element model used for vibration analysis.

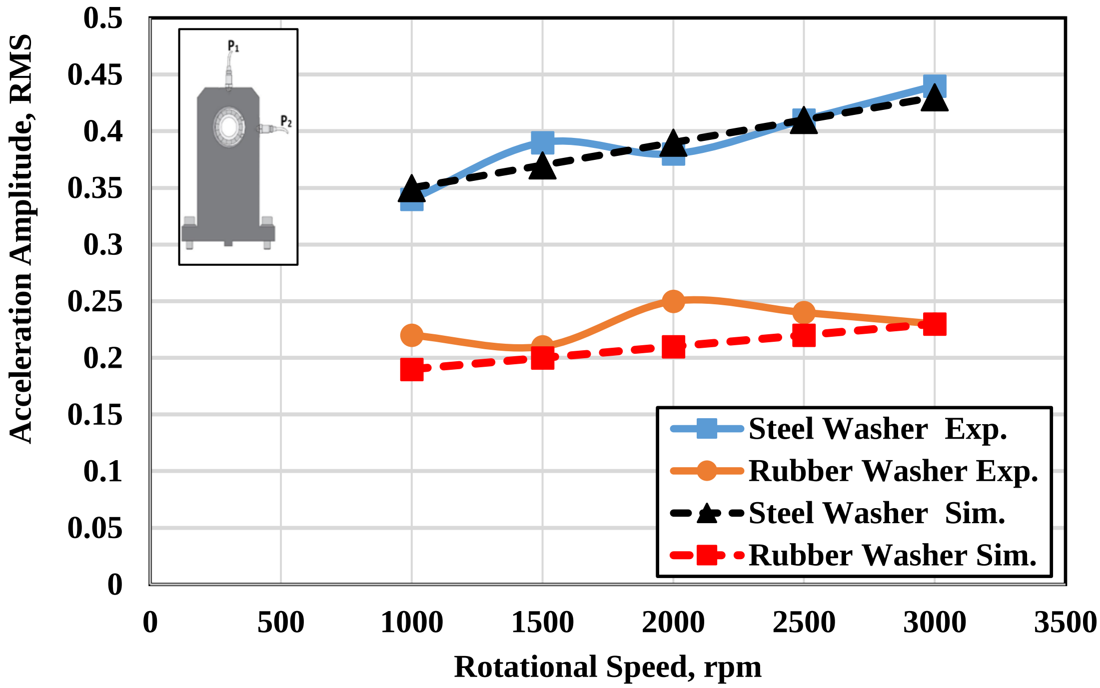


Fig. 10 Comparison between experimental and simulation results.

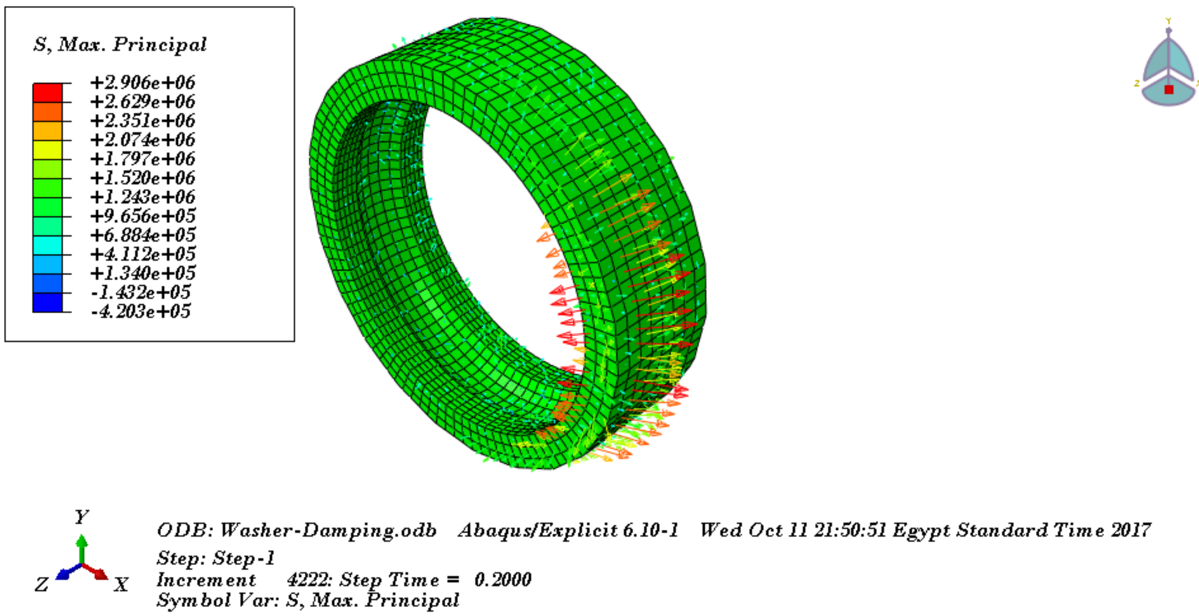


**Fig. 11 Maximum principle stress generated on outer race.**

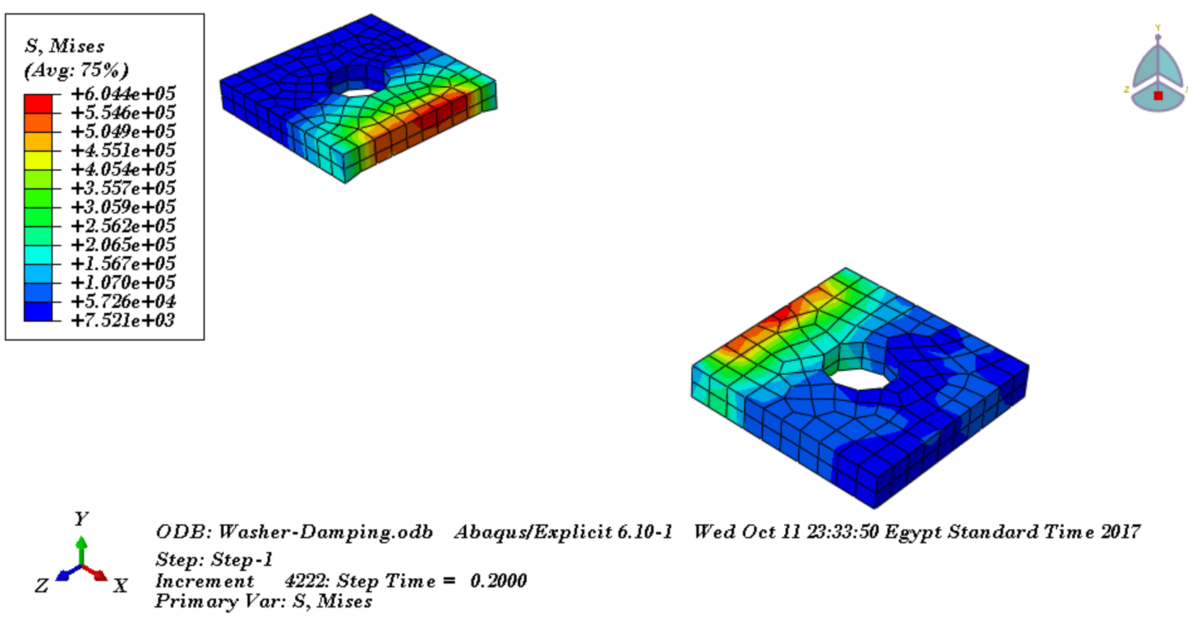


**Fig. 12 Von Mises stress generated on steel washer.**

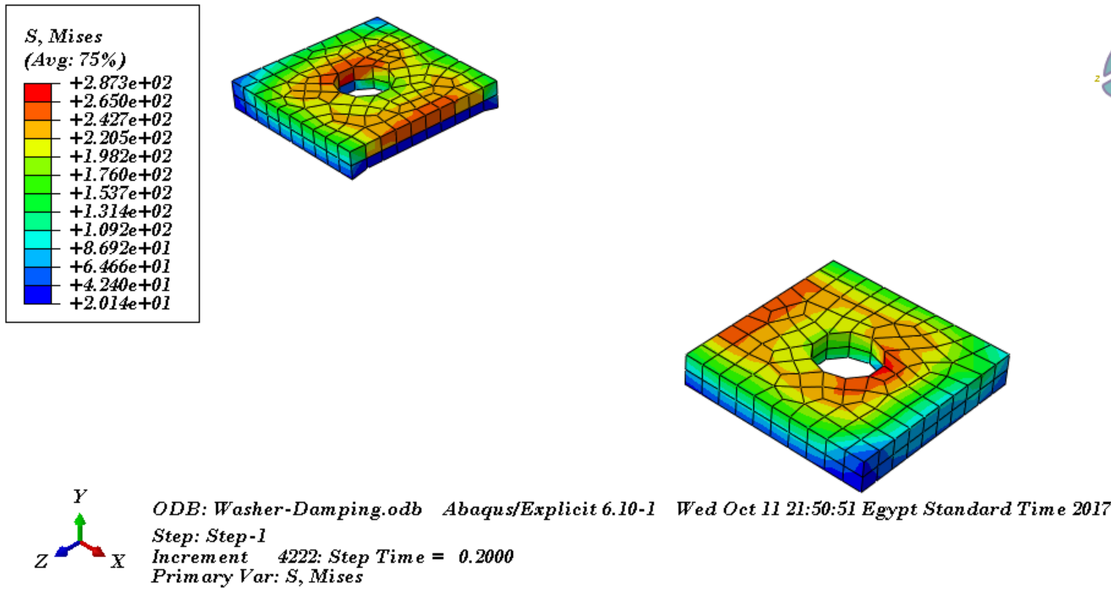


**Fig. 13 Von Mises stress generated on rubber washer.**

**CONCULSIONS**

**More than three quarters of failure events of machine parts are caused by vibration and its related problems; therefore, the Vibration analysis is one of the most important methods used in monitoring damage in mechanical elements. Its low transmissibility means less damage to sensitive components experiencing vibration. It also has vibration isolation properties at large frequency ratios. A rubber washer combines shock absorption, anti-vibration control, and vibration damping to make it the industry leader as an anti-vibration material. The ABAQUS/CAE model developed in this work, shown that the rubber washer, 40 Shore A, (S03) has the best damping factor. On the other hand, the rubber washer has greater ability to dissipate energy generated by vibration and reduces the generated stresses.**

**REFERENCES**

**1. Nabhan, A., Nouby, M., Samy, A.M., Mousa, M.O., "Bearing Fault Detection Techniques -A Review", Turkish Journal of Engineering, Sciences and Technology, Vol. 3 Issue 2, (2015).**

**2. Amarnath M, Shrinidhi R, Ramachandra A, et al. "Prediction of defects in antifriction bearings using vibration signal analysis", IE (I) Journal-MC, Vol. 85, pp. 88 - 92,( 2004).**

**3. Kiral Z and Karagulle H. "Simulation and analysis of vibration signals generated by rolling element bearing with defects", Tribology International, Vol. 36, pp. 667 - 678, (2003).**

**4. Karacay T and Akturk N. "Experimental diagnostics of ball bearings using statistical and spectral methods", Tribology International, Vol. 42, pp. 836 - 843, (2009).**

**5. Kim Y-H, Tan ACC, Mathew J, et al., "Condition monitoring of low speed bearings: a comparative study of the ultrasound technique versus vibration measurements", Proceedings of world congress on engineering asset management (WCEAM), Gold Coast, Australia, London: Springer, pp.182 - 191, (2006).**

**6. Nabhan A., Nouby M., Samy A. M., and Mousa, M. O., "Vibration analysis of deep groove ball bearing with outer race defect using ABAQUS", Journal of Low Frequency Noise, Vibration and Active Control, , Vol. 35 (4), pp. 312 - 325, (2016).**
**7. Kadarno P. and Taha Z. "Vibration analysis of defected ball bearing using finite element model simulation", The 9th Asia Pacific industrial engineering & management systems conference, Bali, Indonesia, (2008).**
**8. Taha Z and Dung N. T. "Rolling element bearing fault detection with a single point defect on the outer raceway using FEA", The 11th Asia Pacific industrial engineering & management systems conference, Melaka, Malaysia, (2010).**
**9. Nabhan A., Nouby M., Samy A. M., and Mousa, M. O., "Multiple Defects Detection in Outer Race of Gearbox Ball Bearing Using Time Domain Statistical Parameters" International Journal of Vehicle Structures & Systems, Vol. 8 (3). pp. 167 - 174, (2016).**
**10. Nabhan A., Nouby M., Samy A. M., and Mousa, M. O., "A Novel Approach for the Effect of the Bearing Housing Height on the Generated Vibration Using Dynamic Model "Journal of the Egyptian Society of Tribology (EGTRIB Journal), Vol. 12(2), pp. 15 - 29, (2015).**
**11. Liu J., Shao Y. and Lim T. C., "Vibration analyses of ball bearings with a localized defect applying piecewise response function", Mechanical Machine Theory, Vol. 56, pp. 156 - 169, (2012).**
**12. Cao H, Niu L and He Z. "Method for vibration response simulation and sensor placement optimization of a machine tool spindle system with a bearing defect", Sensors, Vol. 12, pp. 8732 - 8754, (2012).**
**13. Guo Y. and Parker R. G., "Stiffness matrix calculation of rolling element bearings using a finite element/contact mechanics model", Mechanical Machine Theory, Vol. 51, pp. 32 - 45, (2013).**
**14. Patel U. A. and Rajkamal S. "Vibrational analysis of self-align ball bearing having a local defect through FEA and its validation through experiment", International Journal Modern Engineering Research, Vol. 2, pp. 1073 - 1080, (2012).**
**15. Rafsanjania A., Abbasion S., Farshidianfar A., et al., "Nonlinear dynamic modeling of surface defect sin rolling element bearing systems", Journal of Sound and Vibration, Vol. 319, pp. 1150 - 1174, (2009).**
**16. Patela V. N., Tandonb N. and Pandeyc R. K., "Vibrations generated by rolling element bearings having multiple local defects on races", Procedia Technology, Vol. 14, pp. 312 - 319, (2014).**
**17. Nabhan A., Nouby M., Samy A. M., and Mousa, M. O., "Contact Stress Distribution of Deep Groove Ball Bearing Using ABAQUS" Journal of the Egyptian Society of Tribology (EGTRIB Journal), Vol. 12, No. 1, pp. 49 - 61, (2015).**
**18. Muruganatham B., Sanjith M. A., Krishnakumar B., et al., "Roller element bearing fault diagnosis using singular spectrum analysis", Mechanical System Signal Process, Vol. 35, pp. 150 - 166, (2013).**
**19. Sheen Y. T., "An envelope analysis based on the resonance modes of the mechanical system for the bearing defect diagnosis", Measurement, Vol. 43, pp. 912 - 934, (2010).**
**20. Patil M. S., Mathew J., Rajendrakumar P. K., et al., "A theoretical mode to predict the effect of localized defect on vibrations associated with ball bearing", International Journal Mechanical Sci, Vol. 52, pp. 1193 - 1201, (2011).**

**21. Eman A., Nabhan A., Nouby M., and Abd El-Jaber, G. T., "Influence of Adding Contaminants particles to Lithium Grease on the Frictional Coefficient" Journal of the Egyptian Society of Tribology (EGTRIB Journal), Vol. 14 (1), pp. 15 - 29, (2017).**

**22. Nabhan A., "Vibration analysis of adding contaminants particles and carbon nanotubes to lithium grease of ball bearing "The 22-nd International Conference on VIBROENGINEERING – Moscow (Russia), Vibroengineering Procedia, Vol. 8, pp. 28 - 32, (2016).**